

Supplemental Information

Supplemental Figure S1. Neurodegenerative disease pathways are overrepresented in R521C-enriched mRNAs.

(A) List of genes associated with neurodegenerative diseases in R521C-enriched mRNAs.

(B) 3'READS read clusters of R521C-enriched mRNAs encoding respiratory chain complex subunits from two replicates shown in IGV genome browser.

(C) 3'READS read clusters of non-enriched mRNAs from two replicates shown in IGV genome browser.

(D) Poly (A+) RNA read counts negative control scatter plot is generated using two whole-cell replicates. Standard curve is plotted using linear regression. The outlier genes are data points with top 5% WC1/WC2 ratio above (red) or below (blue) the standard curve. Overrepresentation analysis of 5% outlier genes depicted in the scatter plot.

Supplemental Figure S2. Re-analysis of mutant FUS CLIP-seq and RNA-seq datasets reveals preferential binding for respiratory chain complex mRNAs.

(A) CLIP-seq and RNA-seq data from mouse ESCs-differentiated neurons expressing wild-type and R495X mutant FUS were downloaded from GEO datasets GSE106386 and reanalyzed. Scatter plots of length-normalized exon read counts in CLIP-seq (vertical axis) versus RNA-seq (horizontal axis). Enrichment of individual RNA in CLIP-seq were scored based on the distance to the standard curve derived from linear regression. Top 2% CLIP-enriched RNAs are shown in red. Non-enriched RNAs are shown in pale blue. RNAs belong to neither are shown in dark grey. The 2% most depleted (CLIP-seq depleted) RNAs are shown in green. WT: Pearson's correlation test: $R = 0.2858$, $p < 0.0001$; R495X: Pearson's correlation test: $R = 0.5337$, $p < 0.0001$.

(B) Gene ontology overrepresentation analysis of top 2% CLIP-enriched mRNAs in R495X mutant FUS expressing neurons. Bar graphs are shown in $-\log_{10}$ transformed p values for overrepresentation analysis.

- (C) List of RCC mRNAs overrepresented in top 2% R495X CLIP-enriched transcripts.
- (D) Scatter plots depict top 2% CLIP-enriched RCC mRNAs in wild-type or R495X mutant FUS expressing neurons.
- (E) Venn diagram of RNA targets uniquely bound by mutant FUS in CLIP-seq (Hoell et al., 2011) and R521C-enriched targets from RIP-3'READS data in this study. The bar graph displays the overrepresented GO terms of the 18 overlapped RNA targets.

Supplemental Figure S3. Enrichment of insoluble FUS-R521C associated transcripts is not correlated with the density of reported wild-type FUS binding sequences.

- (A) Occurrence of “CGCGC”, “GUGGU” and “GGUG” per nucleotide (motif density) on each IPed poly(A+) transcripts (vertical axis) are correlated with IP enrichment (horizontal axis) from two replicates. Statistics was performed with Spearman correlation test.
- (B) Motif density of mRNAs encoding respiratory chain complex are compared with total poly(A+) RNAs associated with R521C mutant FUS from two replicates. Statistics: Wilcoxon rank sum test.
- (C) Motif density of R521C-enriched poly(A+) RNAs are compared with total poly(A+) RNAs associated with R521C mutant FUS. Statistics: Wilcoxon rank sum test.
- (D) Density of “CGCGC”, “GUGGU” and “GGUG” presented on mRNAs encoding respiratory chain complex and total poly(A+) RNAs associated with R521C mutant FUS were evaluated separately. Statistics: Wilcoxon rank sum test.

Supplemental Figure S4 related to Figure 2.

RT-qPCR analysis of RNAs associated with GFP-tagged wild-type and R521C mutant FUS from the (A) soluble and (B) insoluble fraction. Individual RCC and control transcripts abundance in IP relative to the input fraction are displayed in mean with standard error derived from three independent experiments. Mann-Whitney *U*-test *** $p < 0.001$, **** $p < 0.0001$.

(C) Immunofluorescence of FUS in healthy control (WT) and ALS patient fibroblasts (R495Efs527X).

Supplemental Figure S5. NDUFA5 mRNA co-localizes with mutant FUS aggregates.

(A) HEK293T cells were transfected with GFP-tagged wild-type or R521C mutant FUS for 48 hours. Immunofluorescence-FISH targeting GFP-FUS protein and NDUFA5 mRNA. Scale bar = 10 μ m.

(B) Co-localization analysis of NDUFA5 mRNA and R521C mutant FUS aggregates. Arrows indicate the aggregates used for intensity profile analysis. Green: GFP-FUS; Red: NDUFA5 FISH. Scale bar in insets = 2 μ m.

(C) Co-localization analysis of IGFBP3 mRNA and R521C mutant FUS aggregates. Arrows indicate the aggregates used for intensity profile analysis. Green: GFP-FUS; Red: IGFBP3 FISH. Scale bar in insets = 2 μ m.

(D) Background control images for FISH. Cells were incubated with or without NDUFA5 transcript-specific probes followed by secondary probe hybridization.

Supplemental Figure S6. Expression of ALS mutant FUS or overexpression of wild-type FUS does not repress overall protein synthesis.

(A) Western blot of puromycin-labeled proteins using antibody raised against puromycin. HEK293T were transfected with GFP-tagged wild-type and ALS mutant FUS for 48 hours followed by puromycin labeling assay. Cycloheximide (10 μ g/ mL) was treated 10 minutes prior to puromycin (1 μ g/ mL) labeling. Total protein is shown by ponceau staining. Puro: Puromycin. CHX: Cycloheximide.

(B) Western blot quantification of puromycin-labeled proteins. Puromycin intensity of each lane is normalized to ponceau stain and GFP-transfected control cells. Data is shown in mean \pm s.d. from three independent experiments. Statistics: One-way ANOVA test *** $p < 0.001$.

(C) The top 5% wild-type and R495X mutant FUS CLIP-enriched RNAs identified from GSE106386 datasets are cross compared with ribosome profiling data from the same study. The cross comparison identifies percent ratio of differentially translated genes in top 5% FUS CLIP-enriched transcripts. Cutoff standard: \log_2 (WT or R495X reads count / Ctrl reads count); Down ≤ -0.5 , Up ≥ 0.5 .

Supplemental Figure S7. Endogenous FUS co-purifies with GFP-tagged wild-type and mutant FUS IP.

(A) GFP-tagged wild-type and R521C mutant FUS were expressed in HEK293T cells followed by cell fractionation-immunoprecipitation using GFP antibodies. Endogenous FUS (Endo FUS) was detected using FUS antibody in WB.

(B) R495Efs527X and P525L mutant FUS immunofluorescence using FUS antibody in ALS patient fibroblasts.

Supplemental Figure S8. Expression of ALS mutant FUS or overexpression of wild-type FUS induces mitochondrial dysfunction.

(A) HEK293T cells were transfected with GFP-tagged (WT) and ALS mutant FUS (R521C, P525L, R495X) for 48 hours then incubated with MitoTracker Red CMXRos (100 nM) for 30 minutes. Immunofluorescence of GFP-FUS and mitochondrial network stained by mitotracker. The mitochondrial network is displayed in binary skeletonized images. Scale bar = 10 μ m.

(B) Number of unbranched mitochondria and branched mitochondrial networks of each cell. N >250, Kruskal-Wallis test ****p < 0.0001.

(C) HEK293T were transfected with siFUS for 72 hours followed by extracellular oxygen consumption assay. Measurements were conducted in three replicates. Data is shown in mean with s.d. Unpaired *t*-test ***p < 0.001; AMA: Antimycin A.

(D) MitoSOX fluorescence spectrum in GFP positive cells were detected using FACS analysis. Total of 10000 cells are counted in each condition. The colored peaks indicate MitoSOX intensity distribution of GFP positive cells. The MitoSOX intensity distribution of control cells (grey) is overlapped with MitoSOX intensity distribution of cells expressing WT or ALS mutant FUS. X-axis: MitoSOX intensity; Y-axis: Cell number.

Supplemental Figure S9. Mitochondrial-encoded respiratory chain complex mRNAs are co-IPed with R521C mutant FUS from insoluble fraction.

Genome browser displays 3'READS read clusters aligned to mitochondrial genome from two R521C-IP replicates. (+) indicates plus strand; (-) indicates minus strand.

Supplemental Figure S10. Mutant FUS localizes to mitochondria in ALS patient fibroblasts.

(A) Mutant FUS and G3BP1 immunofluorescence in ALS patient fibroblasts. Fibroblast samples were subjected to airyscan confocal microscopy. Scale bar = 10 um

(B) Mutant FUS, G3BP1 and mitotracker immunofluorescence in ALS patient fibroblasts. Zoom-in images were indicated by the insets. Scale bar = 2 um

(C) Fluorescence intensity histogram of mitotracker, mutant FUS and G3BP1 indicated in the insets of zoom-in images. Horizontal axis indicates distance in micron. Vertical axis indicates fluorescence intensity in arbitrary units.

Supplemental Figure S11. FUS-targeted nuclear-encoded RCC mRNAs show higher enrichment in mitochondrial fraction.

(A) HEK293T were transfected with GFP-tagged wild-type and R521C mutant FUS for 48 hours followed by mitochondrial fractionation. Levels of individual mRNA in mitochondrial fraction are normalized to their total mRNA levels in unfractionated lysates. GAPDH mRNA serves as cytosolic mRNA control for fold change comparison. (B) Actin mRNA serves as negative control.

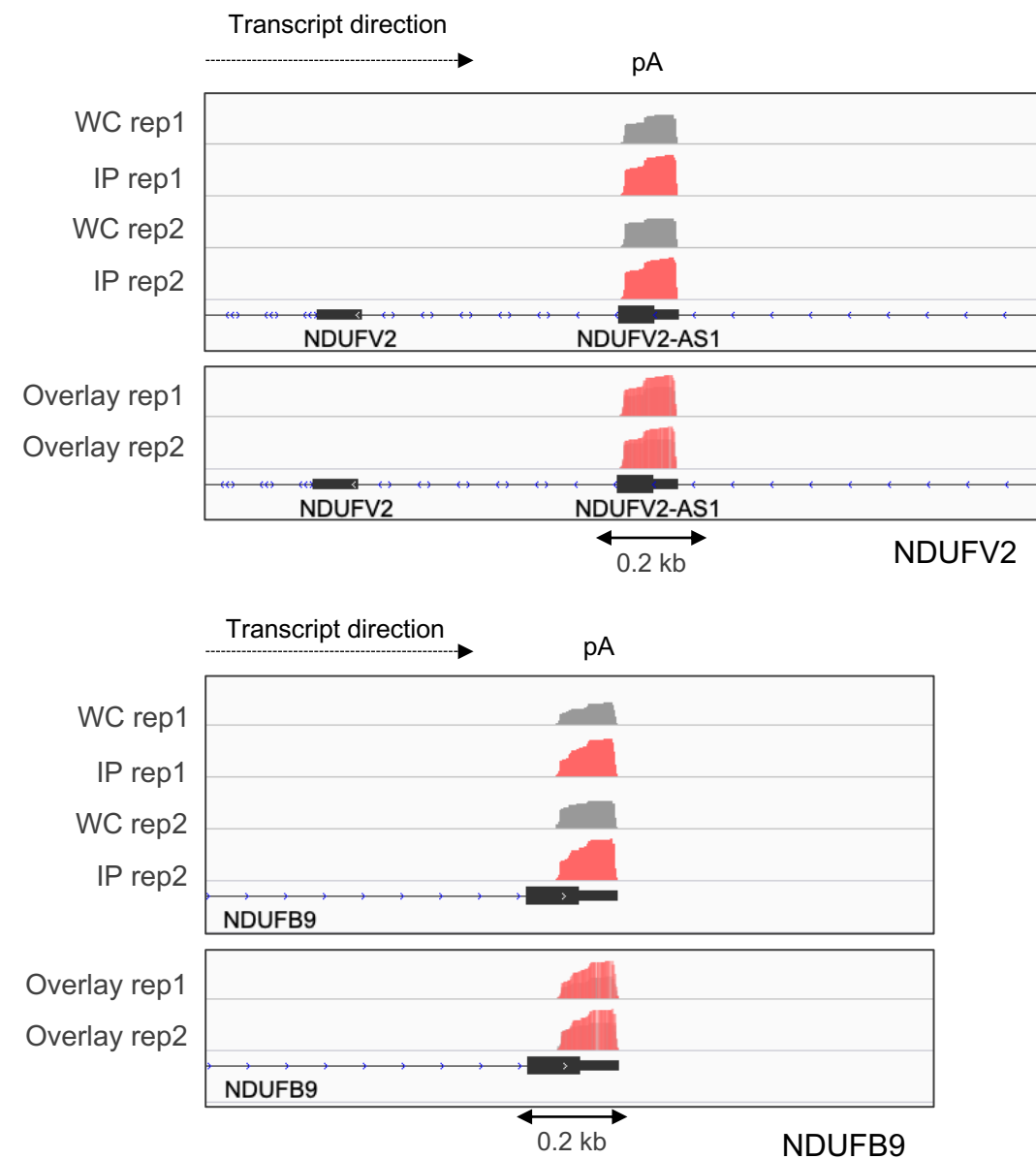
(C) ND1 mitochondrial-encoded mRNA serves as positive control. All bar graphs are shown in mean with s.d. from three independent experiments. Statistics: Unpaired *t*-test * $p < 0.05$, ** $p < 0.01$, *** $p < 0.001$.

A

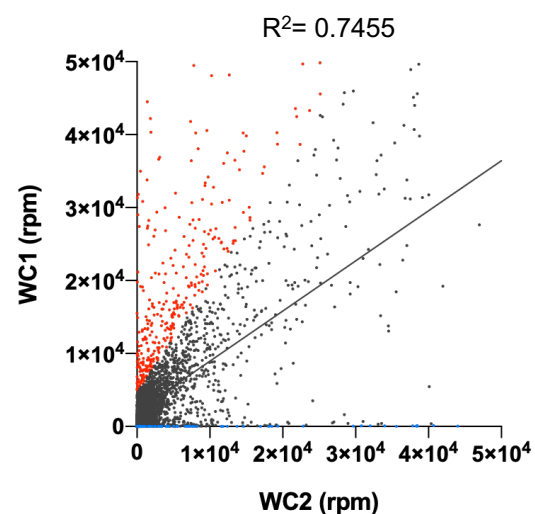
Overrepresented neurodegenerative disease pathways in top 5% R521C-IP enriched mRNAs

Term	Count	PValue	Genes	Fold Enrichment
hsa05012:Parkinson's disease	13	2.23E-06	NDUFA5, NDUFS6, NDUFA2, NDUFS5, COX7A2, UQCRRH, NDUFB9, NDUFV2, COX7A2L, UBE2J2, COX5B, PARK7, ATP5J	5.699
hsa05016:Huntington's disease	14	9.78E-06	NDUFA5, NDUFS6, CLTA, NDUFS5, NDUFA2, COX7A2, UQCRRH, NDUFB9, POLR2J, NDUFV2, COX7A2L, SOD1, COX5B, ATP5J	4.539
hsa05010:Alzheimer's disease	11	3.19E-04	NDUFA5, NDUFS6, NDUFA2, NDUFS5, COX7A2, UQCRRH, NDUFB9, NDUFV2, COX7A2L, COX5B, ATP5J	4.076
Mitochondrial complex I deficiency	3	0.008717676	NDUFS6, NDUFB9, NDUFV2	20.40172166

B

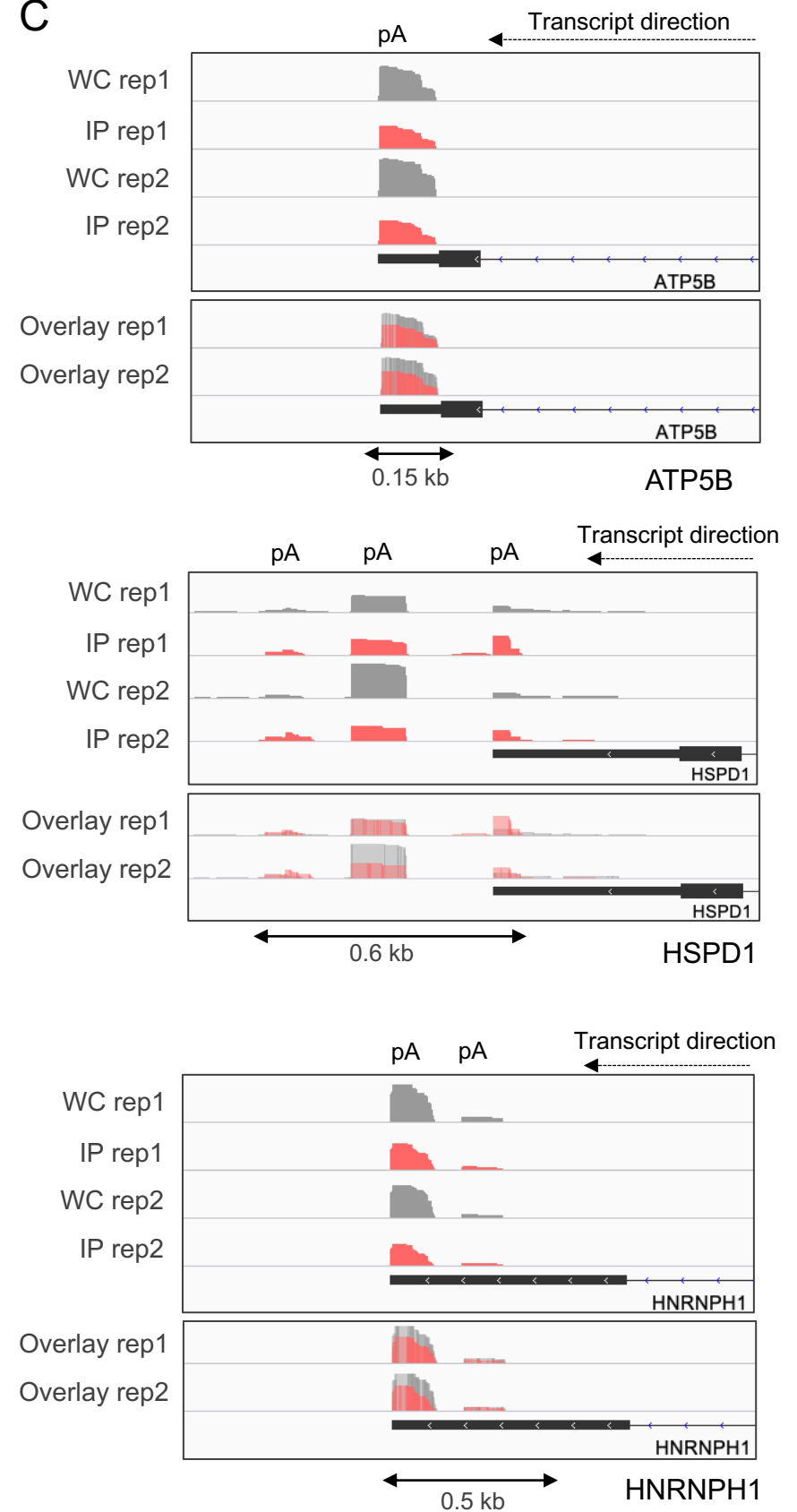


D

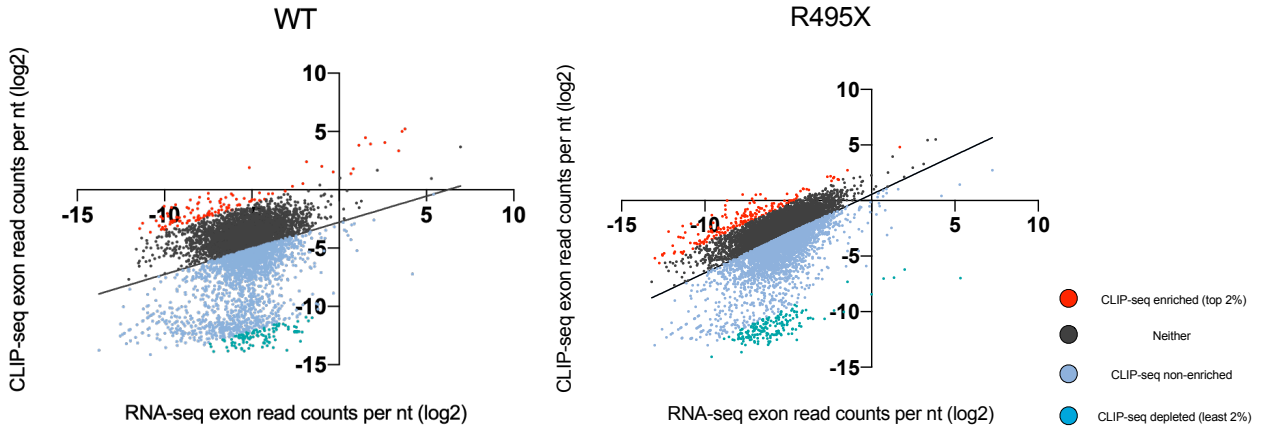


GO terms	Fold Enrichment
proteasome core complex (GO:0005839)	15.19
proteasome complex (GO:0000502)	13.6
cytosolic large ribosomal subunit (GO:0022625)	11
cytosolic small ribosomal subunit (GO:0022627)	10.63
cytosolic ribosome (GO:0022626)	10.53
cytosolic part (GO:0044445)	8.1
coated vesicle (GO:0030135)	6.07
ribonucleoprotein complex (GO:1990904)	3.88
cytosol (GO:0005829)	3.69
cytoplasmic part (GO:0044444)	2.53
cytoplasm (GO:0005737)	2.06
intracellular part (GO:0044424)	2.03
intracellular (GO:0005622)	1.84
cell (GO:0005623)	1.58
cell part (GO:0044464)	1.57
organelle (GO:0043226)	1.47

C

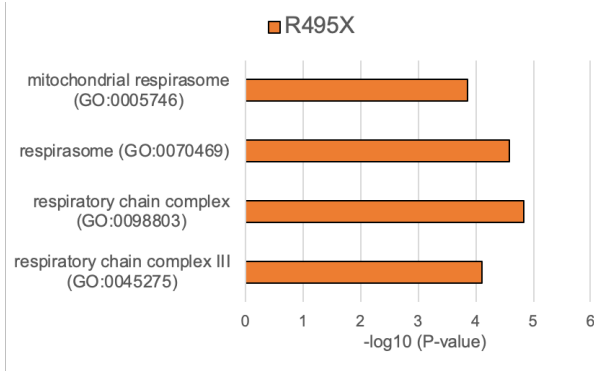


A

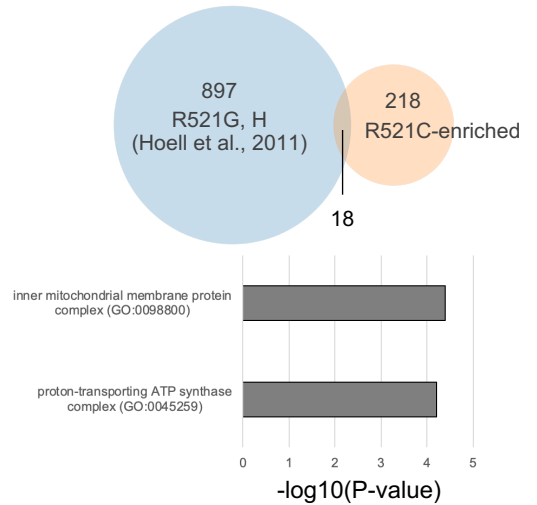


B

CLIP-enriched mRNAs (top 2%)



E

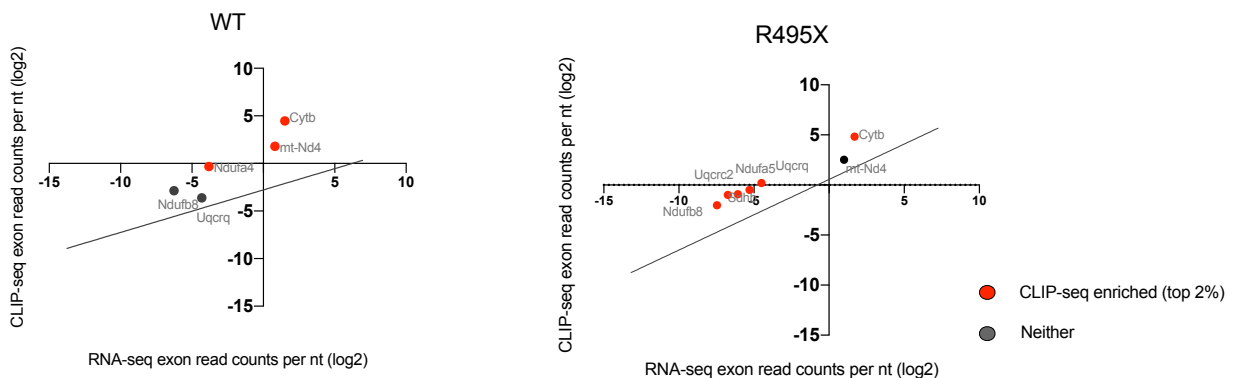


C

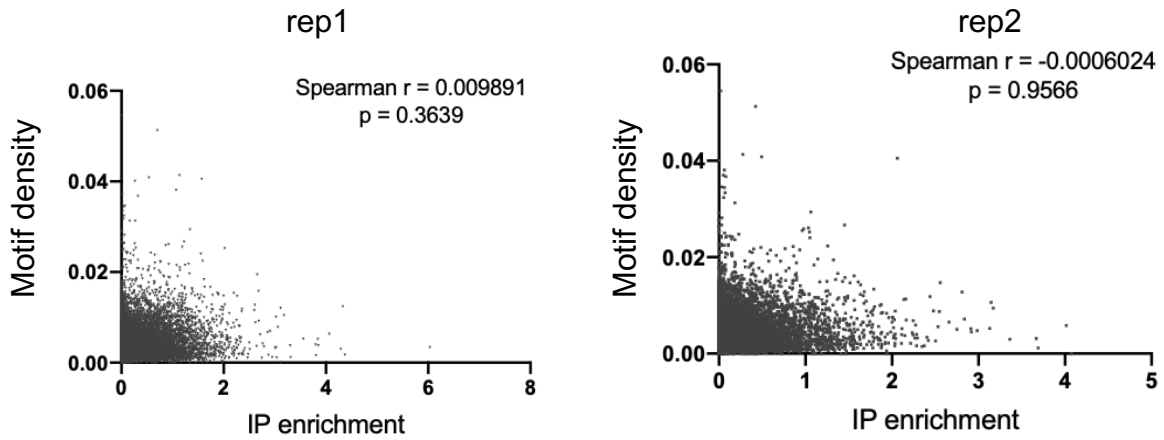
List of respiratory chain complex genes overrepresented in R495X CLIP-enriched mRNAs

respiratory chain complex (GO:0098803)		
MOUSE MGI=MGI=1914514 UniProtKB=Q9D6J5	Ndufb8	NADH dehydrogenase [ubiquinone] 1 beta subcomplex subunit 8, mitochondrial;Ndufb8;ortholog
MOUSE MGI=MGI=1915452 UniProtKB=Q9CPP6	Ndufa5	NADH dehydrogenase [ubiquinone] 1 alpha subcomplex subunit 5;Ndufa5;ortholog
MOUSE MGI=MGI=1914253 UniProtKB=Q9DB77	Uqcrc2	Cytochrome b-c1 complex subunit 2, mitochondrial;Uqcrc2;ortholog
MOUSE MGI=MGI=102501 UniProtKB=P00158	Cytb	Cytochrome b;Mt-Cyb;ortholog
MOUSE MGI=MGI=107807 UniProtKB=Q9CQ69	Uqcrcq	Cytochrome b-c1 complex subunit 8;Uqcrcq;ortholog
MOUSE MGI=MGI=1914930 UniProtKB=Q9CQA3	Sdhb	Succinate dehydrogenase [ubiquinone] iron-sulfur subunit, mitochondrial;Sdhb;ortholog

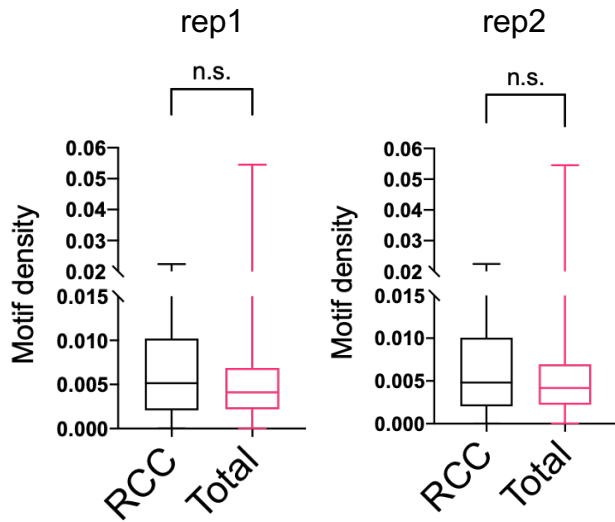
D



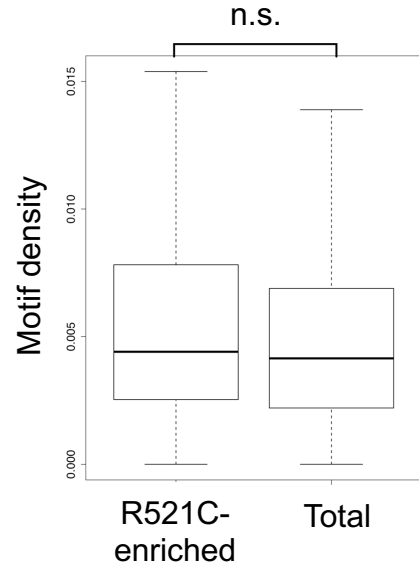
A



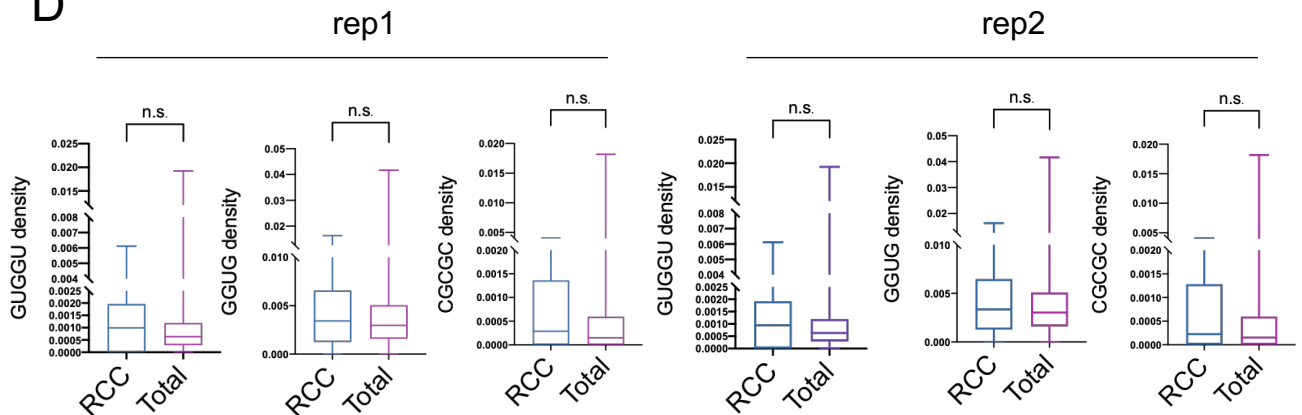
B



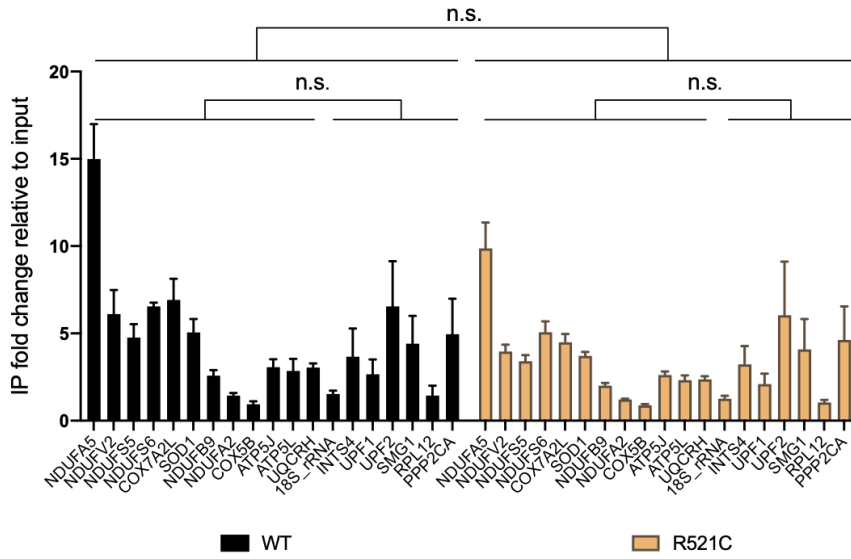
C



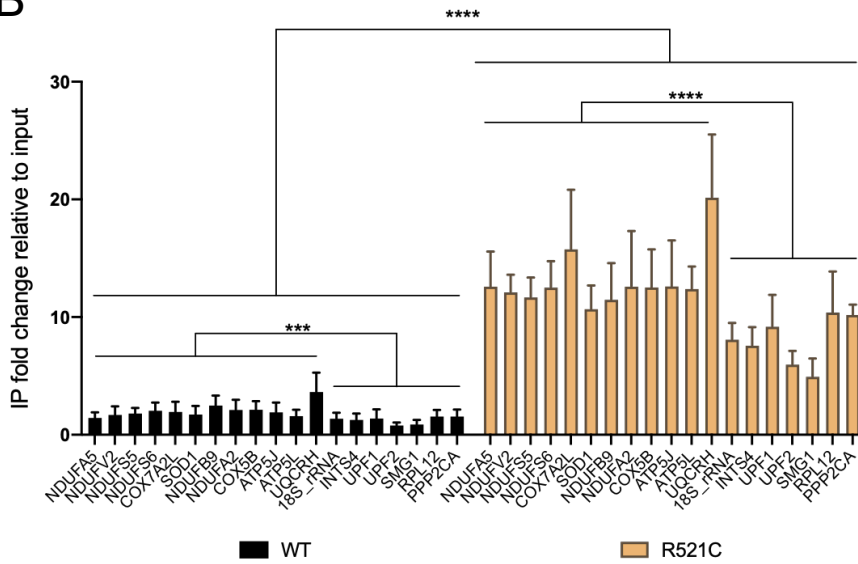
D



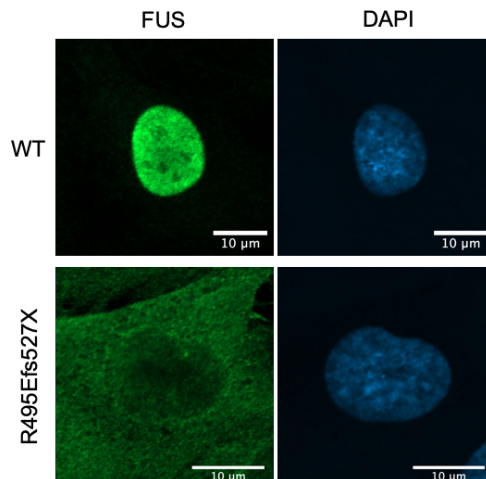
A



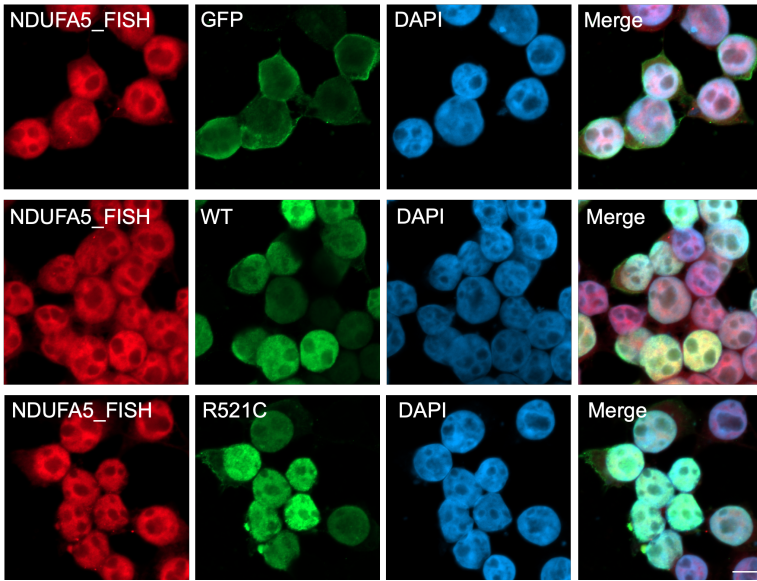
B



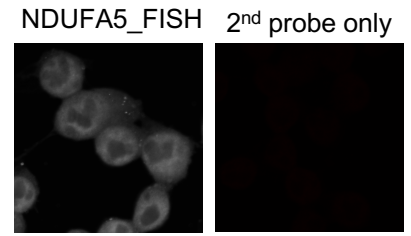
C



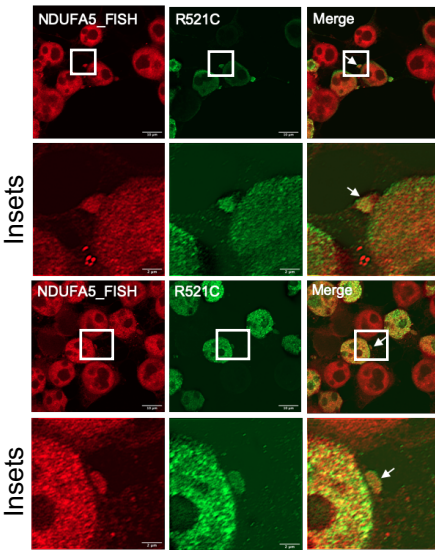
A



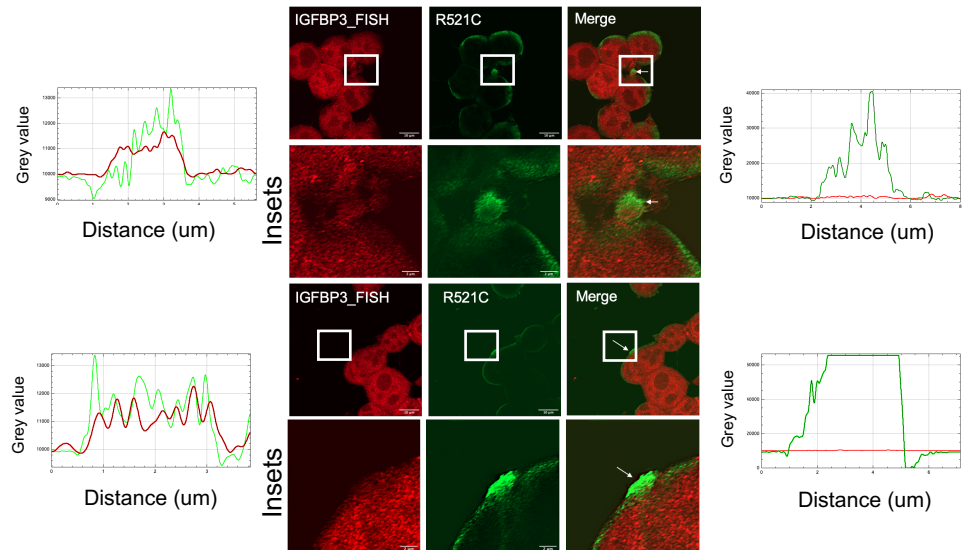
D



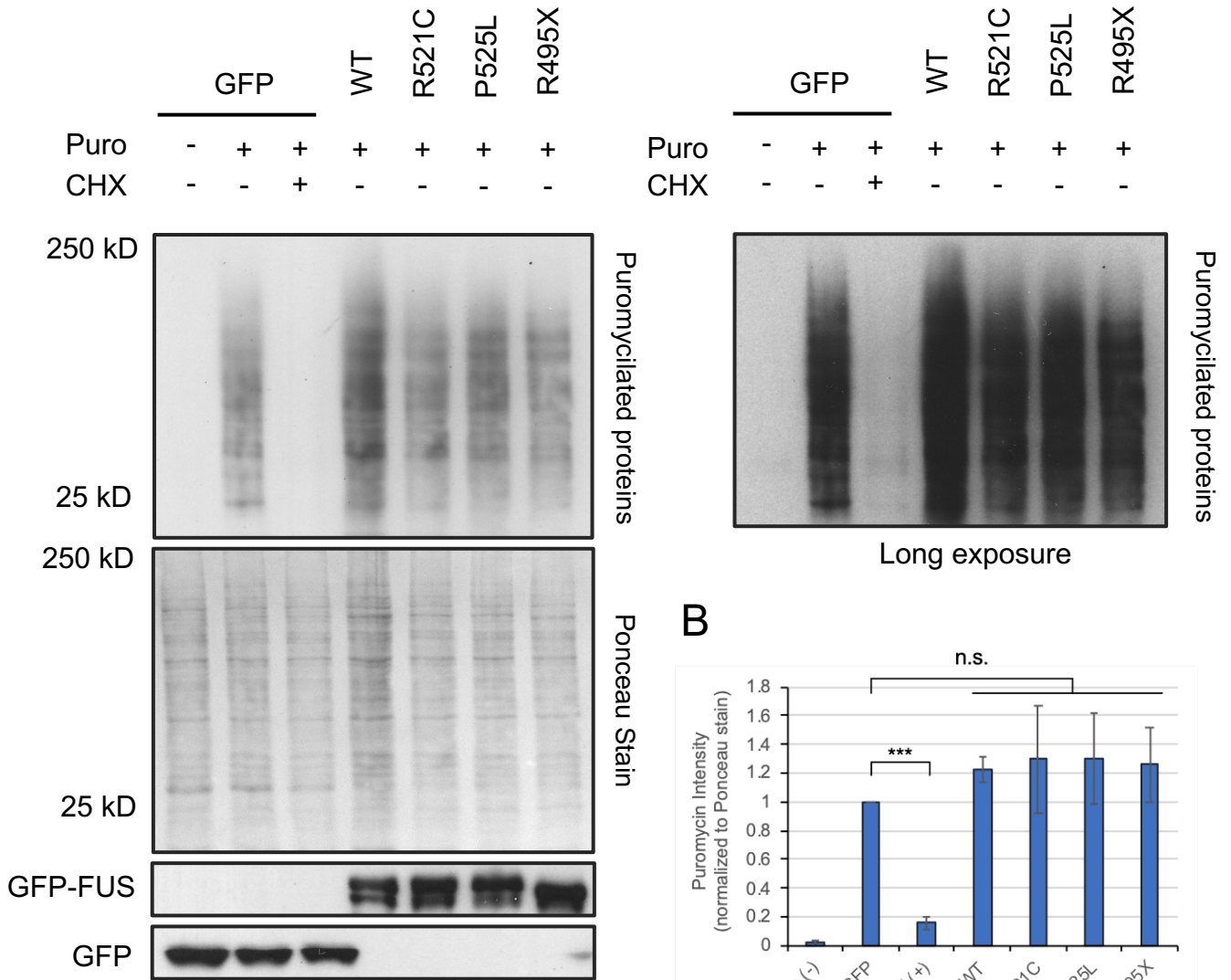
B



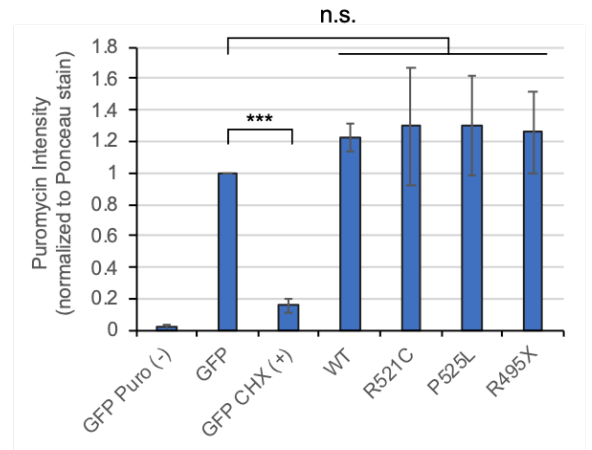
C



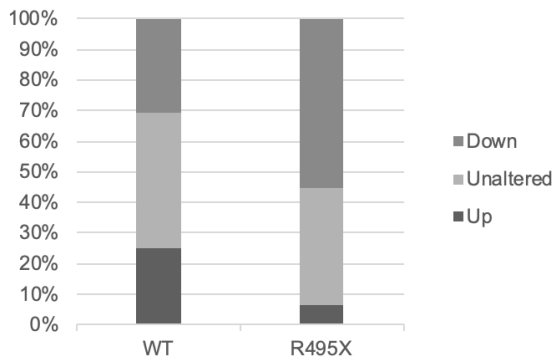
A



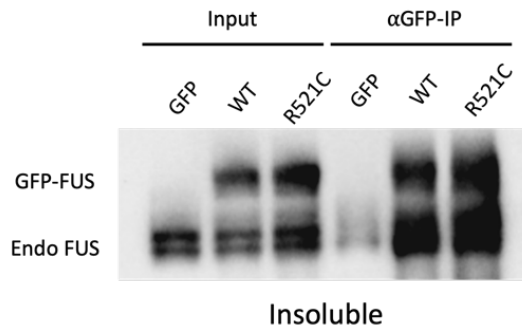
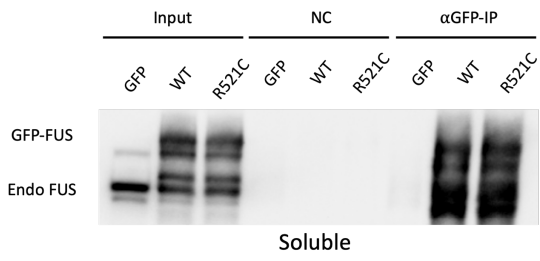
B



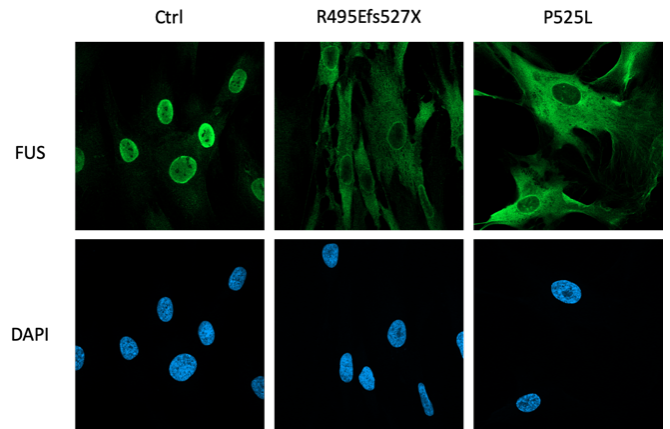
C

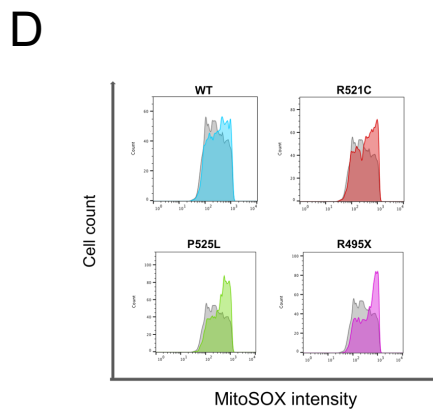
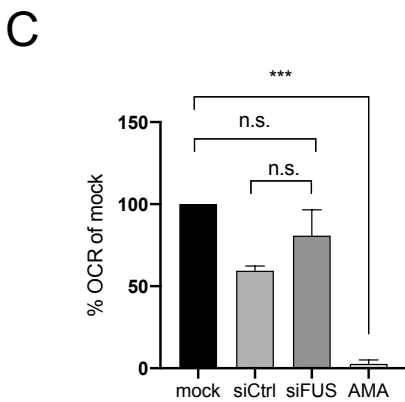
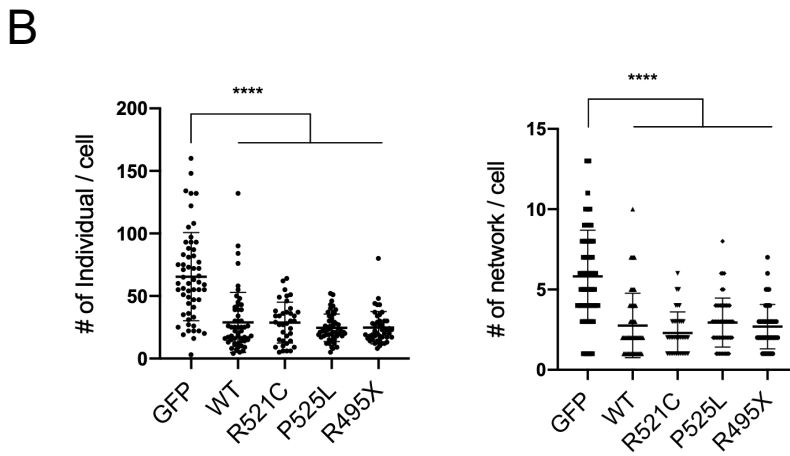
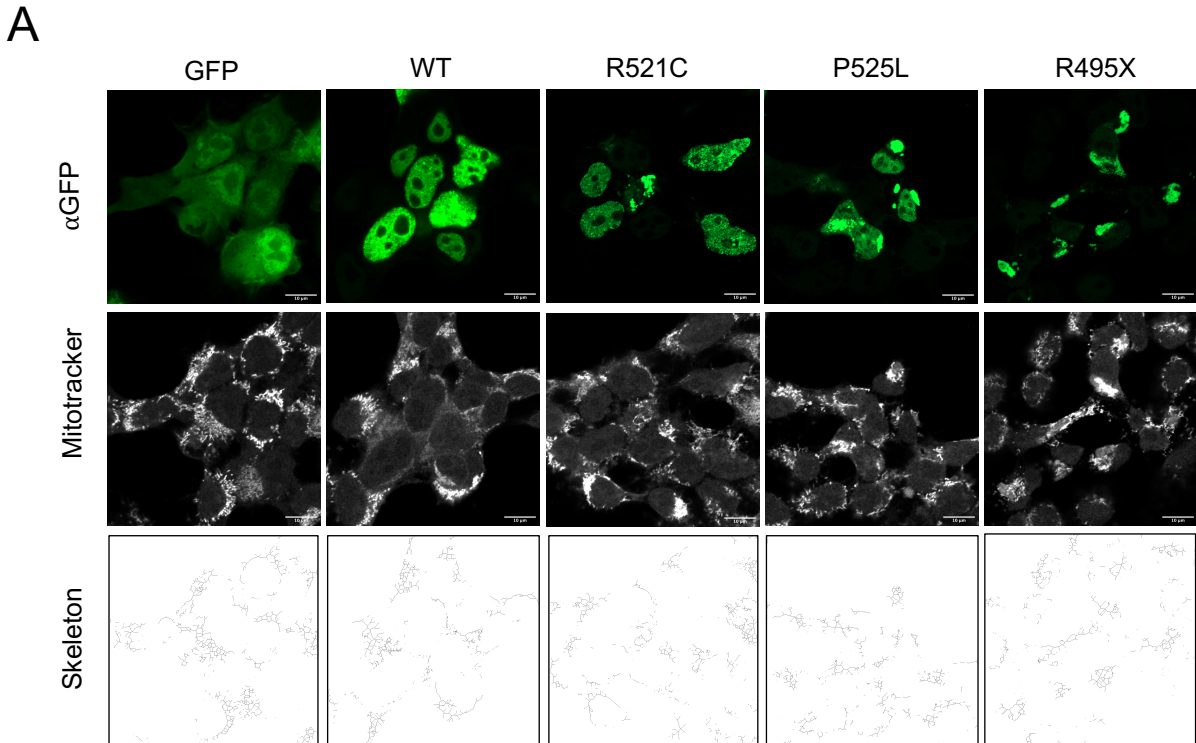


A

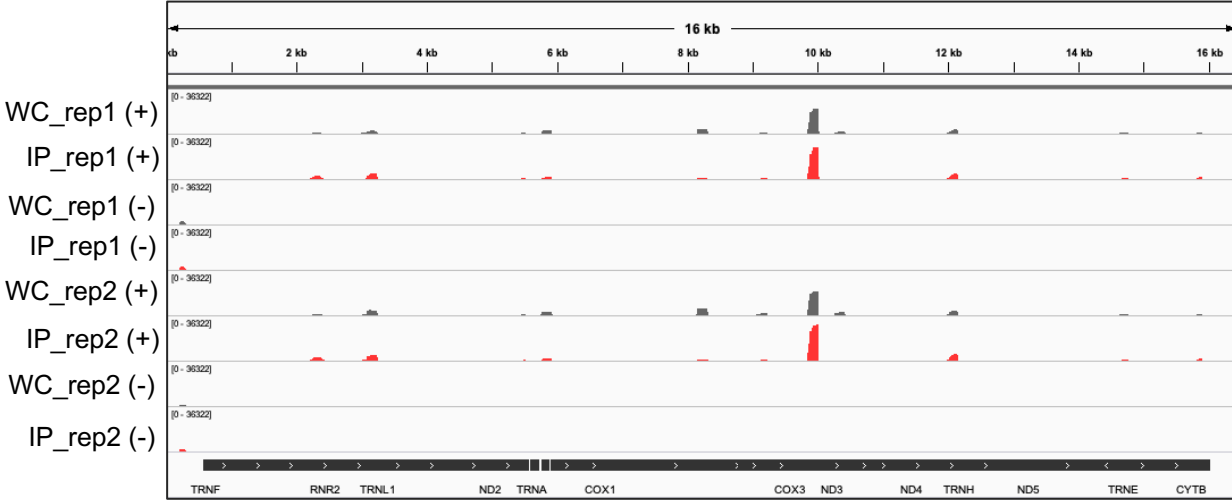


B

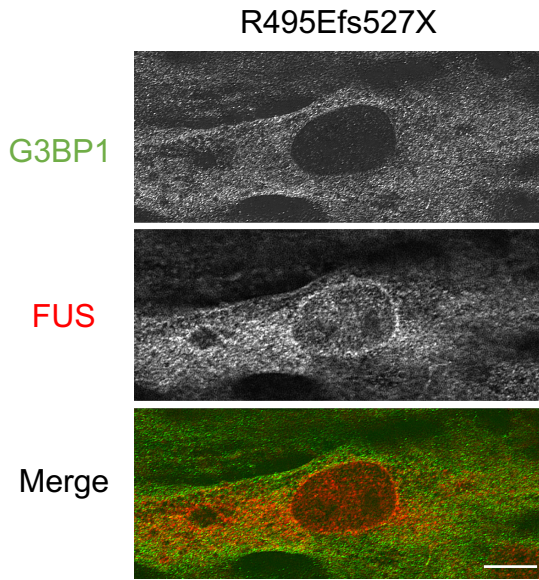




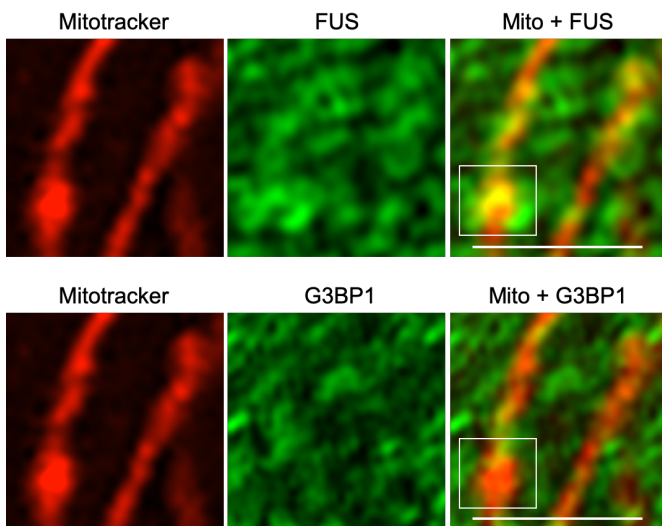
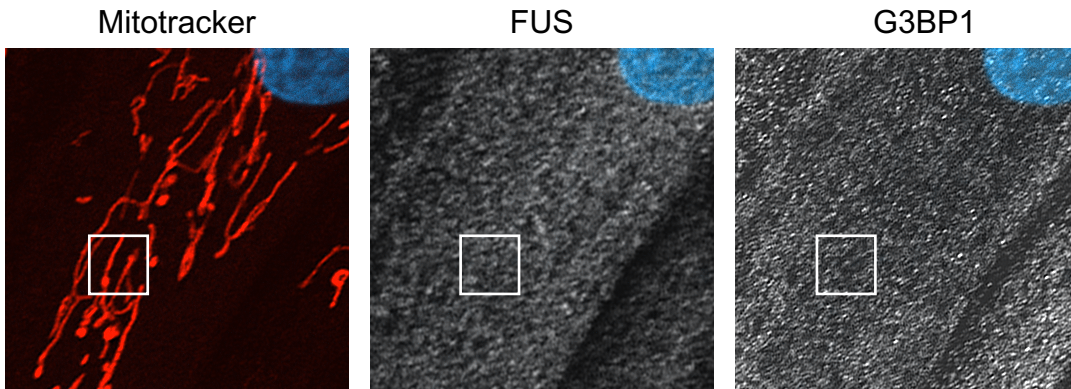
Human mitochondrial genome



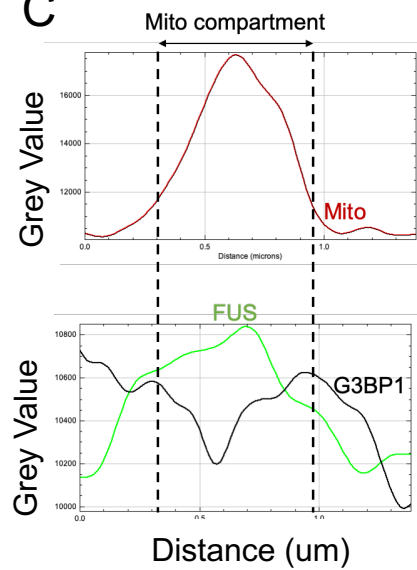
A



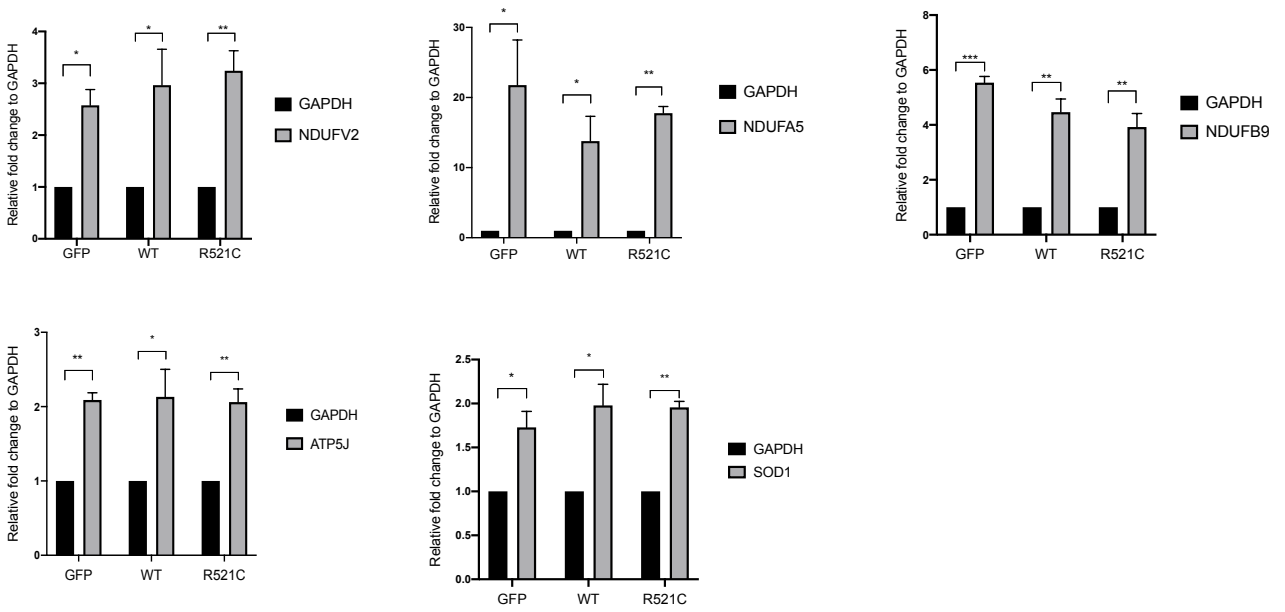
B



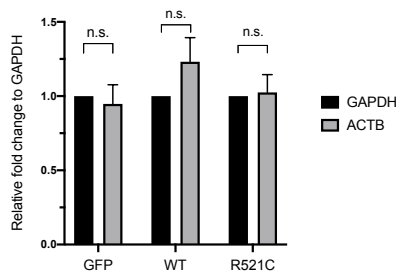
C



A



B



C

